

# Unusual polymerization in the $\text{Li}_4\text{C}_{60}$ fulleride

M. Riccò,\* T. Shiroka, M. Belli, D. Pontiroli, and M. Pagliari  
*Dipartimento di Fisica and Istituto Nazionale di Fisica della Materia,  
Università di Parma, Parco Area delle Scienze 7/a, 43100 Parma, Italy*

G. Ruani and D. Palles†  
*Istituto ISMN-CNR, Via P. Gobetti 101, 40129 Bologna, Italy*

S. Margadonna  
*School of Chemistry, University of Edinburgh, West Mains Road, EH9 3JJ Edinburgh, UK*

M. Tomaselli  
*Laboratory of Physical Chemistry, ETH-Hönggerberg, Pauli Strasse 10, CH-8093, Zürich, Switzerland*  
(Dated: October 17, 2018)

$\text{Li}_4\text{C}_{60}$ , one of the best representatives of lithium intercalated fullerides, features a novel type of 2D polymerization. Extensive investigations, including laboratory x-ray and synchrotron radiation diffraction,  $^{13}\text{C}$  NMR, MAS and Raman spectroscopy, show a monoclinic  $I2/m$  structure, characterized by chains of [2+2]-cycloaddicted fullerenes, sideways connected by single C–C bonds. This leads to the formation of polymeric layers, whose insulating nature, deduced from the NMR and Raman spectra, denotes the complete localization of the electrons involved in the covalent bonds.

PACS numbers: 81.05.Tp, 82.35.Lr, 61.48.+c, 82.56.Ub, 78.30.Na

## I. INTRODUCTION

Extensive investigations of fullerene  $\text{C}_{60}$ , both in its pristine form as well as in its intercalated variants, have definitively confirmed the strong tendency toward polymerization of this molecule. Indeed, the original cubic van der Waals bonded fcc structure of solid  $\text{C}_{60}$  can easily be transformed into 1-, 2-, and even 3-dimensionally connected polymers either by photo-excitation,<sup>1</sup> or by high-temperature and high-pressure<sup>2,3</sup> treatments.

The polymeric forms of  $\text{C}_{60}$  have attracted considerable attention mainly because of the variety of crystal structures and their interesting magnetic, optical and mechanical properties. Notably, ferromagnetism with Curie temperature above 500 K has recently been reported in the rhombohedral phase of the 2D-polymer.<sup>4,5</sup> On the other hand, the intercalation of solid  $\text{C}_{60}$  with electron donors like alkali metals (A), has resulted in a wealth of fulleride salts with stoichiometries  $\text{A}_x\text{C}_{60}$ , among which superconducting  $\text{A}_3\text{C}_{60}$  have received extended attention. The intercalation of alkali metals itself can, in few cases, induce the formation of 1D or 2D arrangements of polymerized  $\text{C}_{60}$ . In particular,  $\text{A}_1\text{C}_{60}$  ( $\text{A} = \text{K}, \text{Rb}, \text{Cs}$ ) can display chains of fullerenes linked by “double” C–C bonds ([2+2]-cycloaddition),<sup>6,7,8</sup> while 1D or 2D arrangements of singly bonded  $\text{C}_{60}$  have been observed in  $\text{Na}_2\text{RbC}_{60}$ <sup>9,10</sup> or  $\text{Na}_4\text{C}_{60}$ .<sup>11,12</sup>

If compared with other better known alkali-doped fullerides, lithium intercalated compounds  $\text{Li}_x\text{C}_{60}$  display quite different properties, which can be mainly ascribed to the small Li-ion dimensions and to the partial charge transfer from the Li-atoms. The most relevant differences, addressed only in recent years,<sup>13,14,15,16,17</sup> concern the large doping range ( $x = 1 \div 30$ ), the lack of su-

perconductivity and the formation of polymerized  $\text{C}_{60}$  structures.<sup>15</sup>

Lithium-doped fullerenes themselves behave differently depending on the amount of intercalated lithium. At high doping levels (typically for  $x > 7$ ) both diffraction<sup>16</sup> and multiple quantum NMR<sup>17</sup> clearly show the formation of lithium clusters located in the largest interstices of the  $\text{C}_{60}$  fcc lattice, with all the members of this subclass having similar properties. However, as the lithium concentration decreases below  $x = 7$ , the volume occupied by the intercalants decreases, while the efficiency of charge transfer is expected to increase. Both these factors lead to a reduction of the inter-fullerene distance, and if two facing carbon atoms get close enough, covalent bonds are formed giving rise to fullerene polymerization.

In this paper we extensively investigate  $\text{Li}_4\text{C}_{60}$ , which is the most representative member of this family by diffraction (laboratory and synchrotron) techniques, as well as  $^{13}\text{C}$  static NMR, magic angle spinning (MAS) NMR and Raman spectroscopy. The polymerization seems to occur as a consequence of the “positive” chemical pressure exerted by Coulomb interaction, leading to a novel 2D polymerization pattern, characterized by the coexistence of single and “double” C–C bonds propagating along two orthogonal directions of the plane. Detailed NMR lineshape analysis and Raman measurements, besides confirming the structure, show beyond doubt the presence of an insulating phase, arising from the electron localization in the covalent bonds.

## II. EXPERIMENTAL METHODS

$\text{Li}_x\text{C}_{60}$  samples ( $1 \leq x \leq 6$ ) were prepared either by thermal decomposition of Li azide or by direct doping with lithium metal. In the former case a mixture of stoichiometric amounts of lithium azide and  $\text{C}_{60}$  powder was heated up to  $\sim 510$  K under dynamical vacuum. In the second case a pellet of metallic lithium and  $\text{C}_{60}$  powder was heated up to  $\sim 540$  K and, after several regrinding and pelleting cycles, a homogeneously doped sample is eventually obtained. Preliminary x-ray characterization showed that both methods yielded good quality samples having the same structure.

Laboratory x-ray diffraction was performed with a Bruker D8 diffractometer equipped with a double Göbel mirror monochromator and a GADDS position sensitive detector (Cu  $K\alpha$  radiation), whereas synchrotron diffraction experiments were performed on the ID31 beamline at ESRF (Grenoble). In both cases the samples were sealed in 0.5 mm quartz capillaries.

An AMX 400 Bruker workstation, equipped for solid state NMR experiments, was used for the static  $^{13}\text{C}$  NMR measurements. The spectra were collected employing a standard Hahn echo pulse sequence ( $90^\circ-\tau-180^\circ$ ) with  $\tau = 100 \mu\text{s}$  and a recycle delay of 200 s. Magic angle spinning (MAS)  $^{13}\text{C}$  NMR measurements were performed with a home-built instrument. In this case the Hahn echo spectra were taken using a  $\tau$  delay equal to twice the rotor period at a spinning rate of 5 kHz and 8 kHz respectively, with a recycle delay of 10 s.

Micro-Raman spectra at room temperature were recorded in a back-scattering geometry using a Renishaw 1000 and a T64000 Jobin-Yvon spectrometers, both equipped with charge coupled device (CCD) cameras and microscope lenses with  $\times 100$  and  $\times 50$  magnification. In both cases the resolution was  $\sim 1.0 \text{ cm}^{-1}$  and the accuracy better than  $0.5 \text{ cm}^{-1}$ . The excitation was provided by the 488.0 nm and 514.5 nm lines of an  $\text{Ar}^+$  laser or the 632 nm line of a He-Ne laser. The laser beam was focused on the sample in a spot of  $\sim 2 \mu\text{m}$  in diameter ( $\times 100$  lens), while the power level was kept below 50  $\mu\text{W}$  to avoid photo-degradation effects. In the adopted scattering geometry the polarization of the incident and scattered light were parallel to each other. Accumulation times of several hours were needed to compensate for the very low levels of scattered light due to the low laser power.

## III. RESULTS AND DISCUSSION

### A. Structural investigation

Laboratory x-ray diffraction measurements were performed on the whole  $\text{Li}_x\text{C}_{60}$  series with  $1 \leq x \leq 6$ . The diffraction patterns show that for  $x \leq 2$  and  $x = 6$  the samples consists of at least two phases, one of which is pristine  $\text{C}_{60}$  which did not take part into the reaction (see

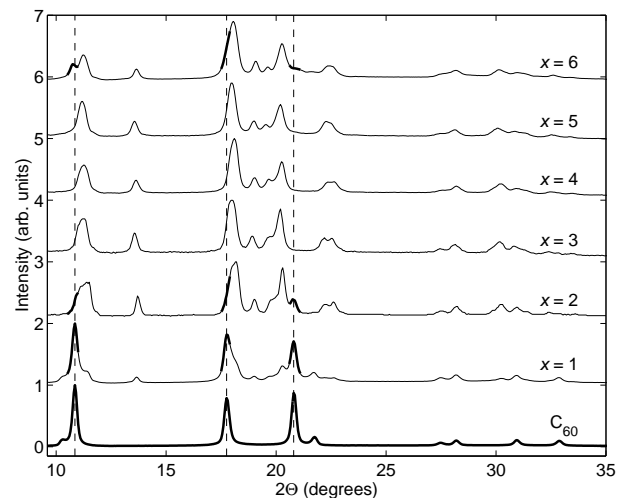


FIG. 1: Room temperature  $\text{Li}_x\text{C}_{60}$  powder diffraction patterns taken with Cu  $K\alpha$  laboratory x-rays for  $1 \leq x \leq 6$ . For  $x = 1, 2, 6$  there is a clear phase co-existence (bold lines), whereas for  $3 \leq x \leq 5$  the samples are homogeneous. For comparison the pristine  $\text{C}_{60}$  diffraction profile and its main peak positions (dashed lines) are also shown.

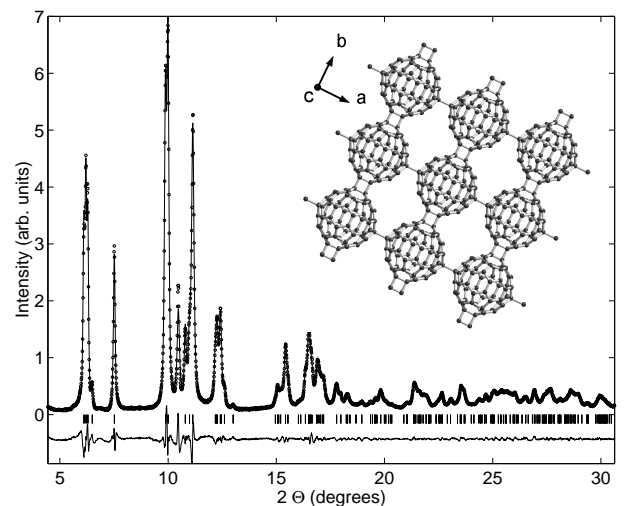


FIG. 2: Measured (o) and calculated (solid line) diffraction pattern of  $\text{Li}_4\text{C}_{60}$  at 300 K. The lower solid line shows the difference profile and the ticks mark the reflection positions. Inset: the polymeric structure of  $\text{Li}_4\text{C}_{60}$ .

Fig. 1). On the other hand, for intermediate stoichiometries  $3 \leq x \leq 5$ , the compounds appear homogeneous and with the same structure. In fact, unlike other alkali doped fullerenes (as e.g.  $\text{K}_x\text{C}_{60}$ ), where the presence of line phases is observed, the structural properties of  $\text{Li}_x\text{C}_{60}$  seem to depend weakly on stoichiometry. Since  $\text{Li}_4\text{C}_{60}$  is expected to be the most representative member of this family, detailed investigations were performed on samples having  $x = 4$ .

Room temperature synchrotron radiation diffraction of  $\text{Li}_4\text{C}_{60}$ <sup>18</sup> (see Fig. 2) shows that its structure is body

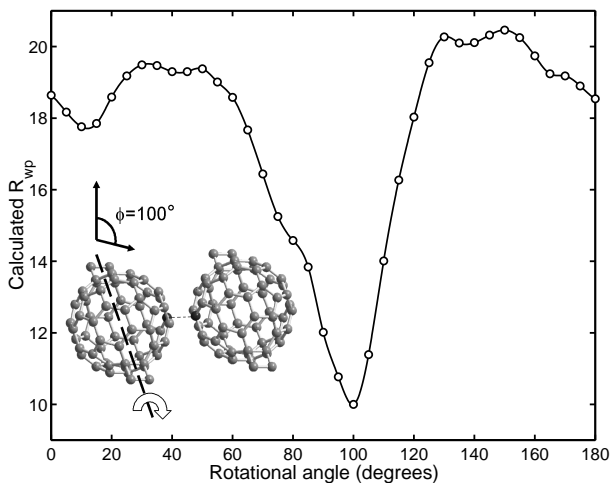


FIG. 3: Fit residuals  $R_{wp}$  as fullerene chains rotate along the  $b$  axis. The minimum at  $\sim 100^\circ$  corresponds to neighboring C atoms facing each other and giving rise to single bond polymerization (see inset).

centered monoclinic (space group  $I2/m$ ) with the following lattice parameters and angle:  $a = 9.3267(3)$  Å,  $b = 9.0499(3)$  Å,  $c = 15.03289(1)$  Å,  $\beta = 90.949(3)^\circ$ . The analysis with the Le Bail pattern decomposition technique provides  $R_{wp} = 4.24\%$  and  $R_{exp} = 1.53\%$ . If center-to-center distances between the nearest  $C_{60}$  units are considered, it turns out that along the  $b$  direction the contact distance ( $\sim 9.05$  Å) is similar to that encountered in other polymerized  $A_1C_{60}$ , thus suggesting the presence of two bridging C–C bonds.

The Rietveld refinement, starting from a structure derived from  $RbC_{60}$ , characterized by linear polymeric inter-fullerene chains directed along the  $b$  axis,<sup>19,20</sup> indicates that the fit quality strongly depends on the fullerene arrangement with respect to chain rotations along the  $[010]$  crystallographic directions. In particular, the fit residual  $R_{wp}$  shows a deep minimum when the angle  $\phi$  with the initial direction becomes  $\sim 100^\circ$  (see inset in Fig. 3).

At this angle, the arrangement of  $C_{60}$  molecules is such that *pairs of carbon atoms* on fullerenes belonging to neighboring chains are found very close ( $\sim 2$  Å) to each other. This strongly suggests that for a suitable orientation of the buckyballs not only the usual polymerization via the  $[2 + 2]$ -cycloaddition reaction along  $b$  direction can take place, but also a connection through single C–C bonds along the  $a$  axis is also possible. The minimum  $R_{wp}$  (5.12%) in the final Rietveld analysis was obtained by refining the positions of the whole  $C_{60}$  atoms by the use of soft constrains. It corresponds to a single inter-fullerene bond length of  $1.75(2)$  Å directed along the  $a$  axis and to a bond inclination of  $\sim 2^\circ$  with respect to the  $ab$  plane.

In an effort to localize the lithium atoms positions, the experimental diffraction pattern was investigated us-

ing Fourier analysis. The maxima of the electronic density map show that two lithium ions are located near the pseudo-tetrahedral site at  $(0.416, 0, 0.748)$ , whereas the other two  $Li^+$  ions per fullerene are found in the  $(0.023, 0, 0.380)$  and  $(-0.023, 0, 0.620)$  positions respectively, symmetrically displaced along the  $c$  direction with respect to the center of the pseudo-octahedral site. In both cases the reported values refer to the average lithium positions, as confirmed by the high isotropic temperature factor ( $B_{iso} \sim 11$ ) and the smooth maxima in the Fourier map.

## B. NMR spectroscopy

The uniqueness of the proposed  $Li_4C_{60}$  structure requires a rigorous and systematic proof also by other independent investigations. Static and MAS (Magic Angle Spinning)<sup>13</sup>C NMR measurements provided such a kind of independent evidence which fully confirmed the previous results.

The room temperature static spectrum of  $Li_4C_{60}$ , referenced to tetramethyl silane (TMS), is shown in Fig. 4 along with a reference spectrum of pristine  $C_{60}$ . The line-shape consists of a broad powder pattern, arising from the chemical shielding tensor, and a relatively narrow peak at lower frequencies which, at the intrinsic resolution of the static spectrum, does not exhibit any peculiar feature. The broad pattern is located in a frequency domain commonly attributed to  $sp^2$  hybridized carbon atoms, whereas the narrow peak falls in the region of  $sp^3$  carbons.<sup>21</sup>

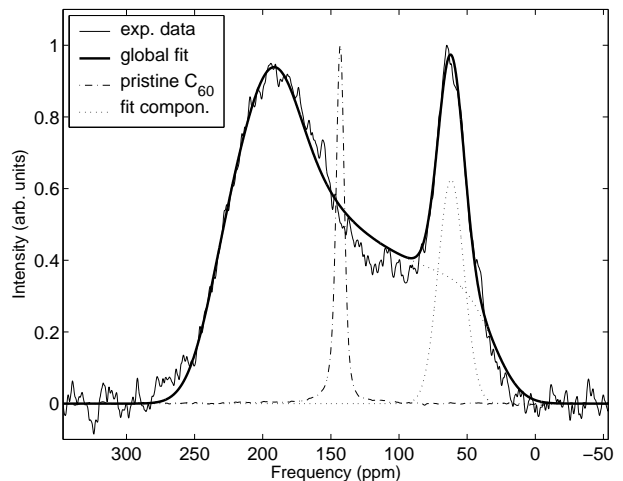


FIG. 4:  $^{13}C$  static NMR spectrum of  $Li_4C_{60}$  at room temperature along with the global fit and its two components (a Gaussian function and a chemical shielding powder pattern). The narrow peak of pristine  $C_{60}$  at 143 ppm is also shown.

The lack of motional narrowing, typically observed in the room temperature  $C_{60}$  rotator phase, indicates that in the as-prepared  $Li_4C_{60}$  the fullerene molecules are ro-

tationally frozen. At the same time, the presence of an  $sp^3$  peak at  $\sim 60$  ppm confirms the formation of covalent bonds among  $C_{60}$  units. A rough estimate of the number of carbon atoms involved in the bonds can be obtained by analyzing the integrated intensity of the different components of the spectrum. To this aim the spectra were fitted with a simple model, comprising a single chemical shift tensor pattern and an additional Gaussian peak. The ratio of the integrated intensities of the two fit components is respectively 1 : 8(1), a result which is in good agreement with the expected 1 : 9 ratio (6 carbon atoms involved in the bonds and 54  $sp^2$ -hybridized carbons per  $C_{60}$  molecule).

A more detailed analysis of the  $sp^2$  component was not possible, since the contributions arising from the 14 inequivalent carbon atoms<sup>18</sup> are not resolved in the static spectrum. Nevertheless, the tensor components can be considered as a rough average of the different contributions, enabling us to make useful comparisons with the carbon NMR spectra of other alkali-doped fullerenes. In particular, it is possible to obtain important clues about the nature of the global shift tensor  $\delta$ , which represents the sum of the chemical shielding tensor  $\sigma_{CS}$ , arising from nucleus interaction with the orbital electrons, and the Knight shift tensor  $\mathbf{K}$ , originating from nucleus interaction with the delocalized conduction electrons. Thus, information about the electronic transport properties of  $Li_4C_{60}$  can be directly extracted from the  $^{13}C$  NMR measurements.

For an easier interpretation, the fitted  $\delta$ -tensor components  $[\delta_{xx} \ \delta_{yy} \ \delta_{zz}] = [237 \ 191 \ 31]$  can be conveniently separated into an isotropic part  $\delta_{iso} = (\delta_{xx} + \delta_{yy} + \delta_{zz})/3$  and an anisotropic traceless tensor  $\delta_{aniso} = \delta - \delta_{iso}$  (the convention adopted is  $|\delta_{zz} - \delta_{iso}| \geq |\delta_{yy} - \delta_{iso}| \geq |\delta_{xx} - \delta_{iso}|$ ). As far as the isotropic part is concerned, the value we find in the  $Li_4C_{60}$  case,  $\delta_{iso} = +153$  ppm, is quite close to the isotropic chemical shift value  $\sigma_{iso} = +143$  ppm of pristine  $C_{60}$ ,<sup>22</sup> which, being the pure  $C_{60}$  an insulator, coincides with its  $\delta_{iso}$ . In alkali-doped fullerenes, where the molecule is found as a  $C_{60}^{n-}$  counter-ion,  $\sigma_{iso}$  is expected to increase slightly as a function of doping reaching  $\sim 150$  ppm for  $n = 3$ ,<sup>23</sup> whereas  $K_{iso}$  for conducting fullerenes is  $\sim 40$  ppm.<sup>23,24</sup> The closeness of the measured  $\delta_{iso}$  to that of pure  $C_{60}$  implies the lack of an *isotropic* Knight shift in the static spectrum of  $Li_4C_{60}$ , a conclusion that is fully consistent with the MAS results (*vide infra*).

On the other hand, a contribution arising from the *anisotropic* part of the Knight shift is still possible. The traceless component of the fitted tensor is  $[84 \ 38 \ -122]$ , implying an anisotropy parameter  $\Omega = \delta_{zz} - \delta_{iso} = -122$  ppm. The traceless tensor represents the sum of the traceless chemical shielding tensor  $\sigma_{aniso}$  and the traceless Knight shift tensor  $\mathbf{K}_{aniso}$ , generally opposite in sign (we assume that the principal axes coincide for the two tensors). Typical values for chemical shielding anisotropy defined as  $\Omega_{CS} = \sigma_{zz} - \sigma_{iso}$  in alkali-metal doped fullerenes fall around -110 ppm (and do not differ signifi-

cantly from the chemical shielding anisotropy in pristine  $C_{60}$ ),<sup>22</sup> while in metallic fullerenes  $\Omega_K$  goes from +160 up to +200 ppm.<sup>23</sup> From the comparison of our measurement with the values taken from the literature we conclude that also the Knight shift traceless tensor is negligible for  $Li_4C_{60}$ .

The analysis of both the isotropic and anisotropic components of the  $sp^2$  part of the spectrum represents therefore a convincing proof of the insulating nature of the  $Li_4C_{60}$  polymer at room temperature.

Finally, we note that the complete absence of a sharp peak near +143 ppm, even with long recycle delays, implies the lack of unreacted  $C_{60}$  in the sample, in agreement with the single phase evidenced by diffraction data.

Further insights come from the  $^{13}C$  MAS spectrum, where the anisotropy of the different interactions is averaged out, just like in NMR in solutions, and only the isotropic shifts are measured.

A MAS measurement on  $Li_4C_{60}$  using an 8 kHz spinning rate is reported in Fig. 5. The spectrum consists of a rather broad  $sp^2$  multiplet, spanning the region from  $\sim 85$  MHz up to  $\sim 210$  MHz, and two well resolved peaks in the  $sp^3$  hybridized carbon region, at +57 ppm and +62 ppm respectively. By comparing the present spectrum with that obtained at a lower spinning rate (5 kHz, not shown here) allowed us to identify the satellite lines of the  $sp^2$  multiplet with the region which includes the small peaks from  $\sim 210$  ppm to  $\sim 300$  ppm and the broad basis below the two  $sp^3$  peaks. On the other hand, the satellite lines originating from the  $sp^3$  peaks had a negligible amplitude and were not considered.

The relatively close spacing of the  $sp^2$  multiplet components, along with the low spinning rate imposed by geometrical constraints, prevented us from unambiguously assigning the  $sp^2$  peaks to each of the 14 structurally inequivalent  $sp^2$  carbon atoms; nevertheless some interesting conclusions can be drawn.

The whole spectrum can be interpreted as follows: the polymerization induces a distortion of the buckyballs, thus different  $sp^2$  carbon atoms are characterized by slightly different isotropic chemical shifts, clearly visible in the MAS spectrum. On the other hand, the two different peaks in the  $sp^3$  carbon region are reminiscent of the two different kinds of covalent bonds, which we can easily identify with the single bond along the *a* direction and the four-membered carbon ring, analogous to a “double” bond, along the *b* direction. Indeed, the integrated intensity ratio of these peaks is approximately 1 : 2, in agreement with the number of carbon atoms involved in the bonds. Moreover, the lower frequency of the smaller  $sp^3$ -like peak reflects its single bond nature, since in this case the more spherical hybridization acts as a better shield to the external field.

As a conclusion, both static and MAS  $^{13}C$  NMR data fully support not only the presence of polymerization in  $Li_4C_{60}$ , but also the complex and unusual bonding motif among the buckyballs. In addition to carbon NMR we performed also  $^7Li$  static NMR measurements.<sup>25</sup> The

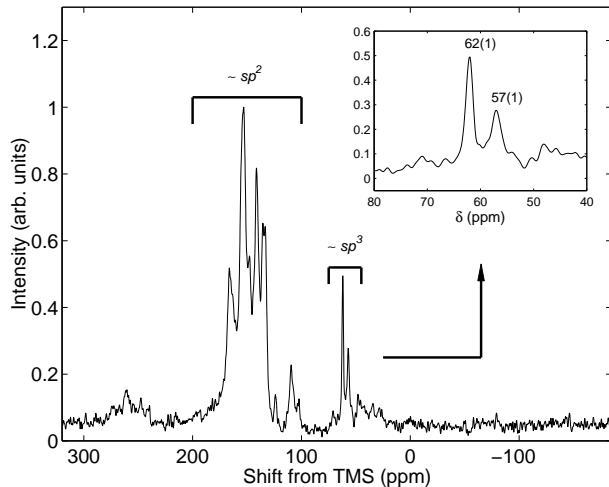


FIG. 5:  $^{13}\text{C}$  MAS (8 kHz) spectrum at 300 K showing the different intensities for  $sp^2$  and  $sp^3$  carbon atoms. Inset: the two peaks in the  $sp^3$  region arise from two different types of  $\text{C}_{60}$  polymerization.

room temperature spectrum (not shown here) consisted of a single peak with an isotropic shift of approximately  $-1$  ppm with respect to a saturated  $\text{LiCl:aq}$  reference solution. The nutation angle analysis led to the conclusion that it is a motionally narrowed peak, confirming once more the rather high mobility of Li atoms at room temperature and the fact that x-ray diffraction can only identify their average positions.

### C. Raman spectroscopy

The presence in fullerenes of ten Raman active modes (the  $A_g$  and  $H_g$  modes) makes Raman spectroscopy one of the preferred tools to study their dynamical and structural properties.<sup>26,27</sup> In a crystal, however, the selection rules derived from the high icosahedral symmetry of  $\text{C}_{60}$  are somewhat relaxed, and several of the previously forbidden modes acquire Raman activity. It is on some of these ‘new’ lines, which have become fingerprints of solid state phenomena like polymerization and dimerization, where we focus our attention.

In the Raman spectra of undoped polymeric  $\text{C}_{60}$ , the double peak in the region  $940\text{--}980\text{ cm}^{-1}$  has been assigned to the stretching vibrations of the four carbon atoms participating in the bridging [2+2] bonds between neighboring  $\text{C}_{60}$  cages and is considered as a signature of polymeric  $\text{C}_{60}$ .<sup>28</sup> Indeed, it is present both in the tetragonal<sup>29</sup> ( $946$  and  $974\text{ cm}^{-1}$ ,  $\Delta\omega = 28\text{ cm}^{-1}$ ) as well as rhombohedral<sup>4</sup> ( $959$  and  $978\text{ cm}^{-1}$ ,  $\Delta\omega = 19\text{ cm}^{-1}$ ) phases of  $\text{C}_{60}$ . Nevertheless, the surprising presence of similar peaks ( $966$  and  $980\text{ cm}^{-1}$ ,  $\Delta\omega = 14\text{ cm}^{-1}$ ) also in the polymerized *single* C–C bond  $\text{Na}_4\text{C}_{60}$ ,<sup>29</sup> with a monoclinic two-dimensionally linked structure, has put serious doubts on the exclusive assignment of these peaks

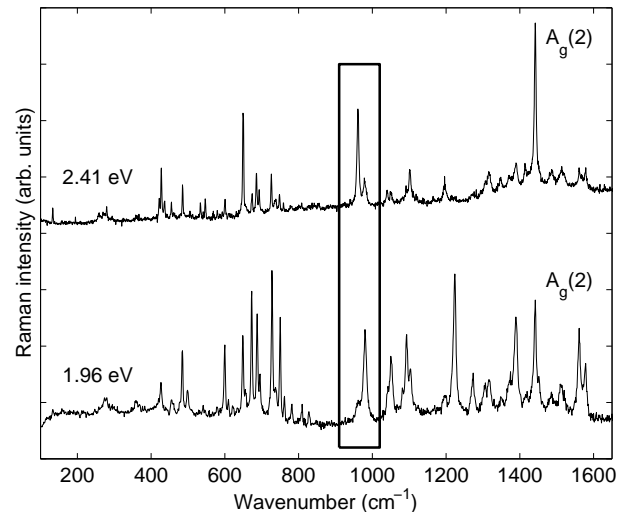


FIG. 6: Room temperature micro-Raman spectra of  $\text{Li}_4\text{C}_{60}$  in a parallel polarization scattering geometry and for two laser excitation energies: 2.41 eV and 1.96 eV. The two peaks arising from carbon polymerization are shown in the boxed area.

to the ring stretch vibrations. Currently they tend to be associated with the more generic presence of  $sp^3$ -type intermolecular bonds.

The Raman spectra of  $\text{Li}_4\text{C}_{60}$ , synthesized by direct Li metal doping, are shown in Fig. 6. As expected, the presence of polymerization  $sp^3$  bonds gives rise to both the characteristic peaks ( $961\text{ cm}^{-1}$  and  $979\text{ cm}^{-1}$ ,  $\Delta\omega = 18\text{ cm}^{-1}$ ), with positions and splitting very similar to those of rhombohedral  $\text{C}_{60}$ . Differently from what is found in the  $\text{Na}_4\text{C}_{60}$  case, though, where both peaks have similar amplitudes and their relative heights do not change with laser excitation energy, in our case the analogous peak heights depend strongly on laser wavelength (see boxed area in Fig. 6). This can be easily rationalized if the complete equivalence of carbon bonds in the first case, and their mixed nature in the latter, is taken into account.

A further confirmation about the lowered symmetry of the mixed polymeric structure, due to the presence of single bonds in one direction and ‘‘double’’ C–C bonds in the orthogonal direction, as well as to a possible crystal field distortion due to the intercalated Li atoms, is found in the increased complexity of the Raman spectrum. Indeed, in the low symmetry crystal structure of  $\text{Li}_4\text{C}_{60}$  at least 41 discernible bands can be recognized, to be compared with e.g. the higher symmetry tetragonal polymeric  $\text{C}_{60}$ , with only  $\sim 23$  discernible bands (excluding very weak ones).<sup>29</sup> Moreover, also three low energy modes (which are silent in the highly symmetric crystalline  $\text{C}_{60}$ ) and attributed to intramolecular stretching are observed as well at  $133$ ,  $158$  and  $195\text{ cm}^{-1}$ .

The Raman spectra of  $\text{Li}_4\text{C}_{60}$  are generally characterized by narrow peaks, indicating both an ordered structure and a negligible electron phonon interaction, as in the case of non metallic systems.<sup>30</sup> In particular, the band

assigned to the  $A_g(2)$  parent mode, located at  $1442\text{ cm}^{-1}$  (see Fig. 6), is very narrow ( $< 6\text{ cm}^{-1}$ ), confirming the presence of a single phase fulleride.

Since many of the Raman peaks of  $\text{Li}_4\text{C}_{60}$  appear either in the tetragonal two-dimensional polymeric  $\text{C}_{60}$  (characterized by “double” C–C bonds) or in the monoclinic two-dimensional polymeric network of  $\text{Na}_4\text{C}_{60}$  (characterized by single C–C bonds), we can infer the mixed nature of our sample, in agreement with the results from x-ray diffraction. We point out, however, that although the present Raman spectrum is practically identical to that of  $\text{Li}_4\text{C}_{60}$  reported in Ref. 31, the latter was characterized as a two-dimensional “double” bond polymer.

The energy dependence of the  $A_g(2)$  mode of  $\text{C}_{60}$  (located at  $1469\text{ cm}^{-1}$  for the pristine material) has been correlated approximately linearly with the amount of charge transferred to the  $\text{C}_{60}$  cage for the most studied alkali fullerides,  $A_x\text{C}_{60}$ ,  $A = \text{K}, \text{Cs}, \text{Rb}$ , where the charge transfer has been verified independently using other experimental techniques. In this case an  $A_g(2)$  mode softening by  $6\text{--}7\text{ cm}^{-1}$  per electron transfer has been measured by Raman scattering.<sup>32</sup>

For polymeric  $\text{C}_{60}$ , on the other hand, the issue of charge transfer is complicated by the presence of covalent bonds between  $\text{C}_{60}$  units, which also causes a downshift of the  $A_g(2)$  mode energy. According to the hypothesis reported in Ref. 29, the  $A_g(2)$  mode energy downshift attributable to cage polymerization is  $\sim 2.5\text{ cm}^{-1}$  per single and  $\sim 5.5\text{ cm}^{-1}$  per “double” C–C bond. Under this assumption, the charge transferred to  $\text{C}_{60}$  in the  $\text{Li}_4\text{C}_{60}$  case should be  $[1469 - (2 \times 5.5 + 2 \times 2.5) - 1442]/6 \approx 2e^-$ , presumably arising from only a partial charge transfer. It remains therefore unclear whether the values of the  $A_g(2)$  mode energy in  $\text{Na}_4\text{C}_{60}$  and  $\text{Li}_4\text{C}_{60}$  can indeed be explained by this ‘rule’ or if there exists in the polymeric systems some other mechanism that supersedes this simple additive rule and makes the identical  $A_g(2)$  mode energies a direct consequence of a similar charge transfer in both cases.

It is known that for  $\text{Li}_x\text{CsC}_{60}$ <sup>33</sup> (and in part also for  $\text{Na}_x\text{C}_{60}$ <sup>34</sup>) only an incomplete charge transfer from the alkali to the  $\text{C}_{60}$  molecule takes place, in contrast to what is observed in other alkali metal doped fullerides.

In the case of  $\text{Li}_4\text{C}_{60}$  the large mobility of the Li atoms at room temperature, suggested by NMR measurements, is not compatible with the existence of hybrid electronic states between Li and  $\text{C}_{60}$ . Notably, Raman measurements performed in the high temperature monomeric

phase of  $\text{Li}_4\text{C}_{60}$ , indicate a  $\text{C}_{60}^{-4}$  charge state.<sup>35</sup>

#### IV. CONCLUSIONS

In summary, the combination of powder diffraction analysis, NMR and Raman spectroscopies allowed us to precisely identify the structure as well as to probe the electronic properties of  $\text{Li}_4\text{C}_{60}$ , the best representative of low-doped lithium fullerides. A novel 2D polymeric arrangement with a mixed interfullerene bonding motif was found at room temperature. The formation of [2+2]-cycloaddicted fullerene chains sideways connected with single C–C bonds, suggested by the diffraction, is fully confirmed by NMR and Raman spectroscopy. The former shows two distinct  $sp^3$  lines in the  $^{13}\text{C}$  MAS spectrum whose intensity ratio agrees with the number of carbon atoms involved in the bonds, while the latter shows the presence of a doublet in the  $940\text{--}980\text{ cm}^{-1}$  region, a well known fingerprint of fullerene polymers. Both  $^{13}\text{C}$  and  $^7\text{Li}$  NMR show the absence of Knight shift as well as any paramagnetic shift, clearly indicating that this polymer is a diamagnetic insulator. A measurement of the amount of charge transferred to  $\text{C}_{60}$  from the Raman  $A_g(2)$  mode shift (a widely used method in alkali fullerides) cannot be reliably extended to fullerene polymers, where molecules are deformed by the presence of intermolecular bonds. Empirical rules<sup>29</sup> suggest in  $\text{Li}_4\text{C}_{60}$  only a partial transfer of two electrons, although diffraction Fourier analysis locates Li ions too far from the fullerene molecules to allow the hybridization of the  $2s$  electron (as it was observed also in  $\text{Li}_x\text{CsC}_{60}$ <sup>33</sup>). This puts some doubts on the general application of these rules to different  $\text{C}_{60}$  polymer structures.

#### Acknowledgments

We thank Dr. C. Vignali of the Centro Interfacoltà Misura di Parma University for his valuable help with the static NMR experiments and acknowledge the financial support by the national FIRB project “New Materials and Mechanisms of Superconductivity in Fullerenes”.

D.P. acknowledges the financial support by the European Commission through the T.M.R. network no. ERBFMRX-CT97-0155 “FULPROP” and the Greek State Scholarships Foundation (I.K.Y.).

---

\* Electronic address: Mauro.Ricco@fis.unipr.it;  
URL: <http://www.fis.unipr.it/~ricco/>

† Permanent address: Department of Physics, School of Applied Sciences, National Technical University of Athens, Heron Polytechniou 9 st., 15780 Zografos, Greece.

<sup>1</sup> M. Núñez-Regueiro, L. Marques, J.-L. Hodeau, O. Béthoux,

and M. Perroux, Phys. Rev. Lett. **74**, 278 (1995).

<sup>2</sup> L. Marques, M. Mezouar, J.-L. Hodeau, M. Núñez-Regueiro, N.R. Serebryanaya, V.A. Ivdenko, V.D. Blank, and G.A. Dubitsky, Science, **283**, 1720 (1999).

<sup>3</sup> Y. Iwasa, T. Arima, R.M. Fleming, T. Siegrist, O. Zhou, R.C. Haddon, L.J. Rothberg, K.B. Lyons, H.L. Carter

- Jr., A.F. Hebard, R. Tycko, G. Dabbagh, J.J. Krajewski, G.A. Thomas, and T. Yagi, *Science* **264**, 1570 (1994).
- <sup>4</sup> T.L. Makarova, B. Sundqvist, P. Esquinazi, R. Höhne, Y. Kopelevich, P. Scharff, V. A. Davydov, L. S. Kashevarova, and A. V. Rakhmanina, *Nature* **413**, 716 (2001).
  - <sup>5</sup> R.A. Wood, M.H. Lewis, M.R. Lees, S.M. Bennington, M.G. Cain, and N. Kitamura, *J. Phys.: Condens. Matter*, **14**, L385 (2002).
  - <sup>6</sup> J. Winter and H. Kuzmany, *Carbon*, **36**, 599 (1998).
  - <sup>7</sup> O. Chauvet, G. Oszlányi, L. Forró, P. W. Stephens, M. Tegze, G. Faigel, and A. Jànossy, *Phys. Rev. Lett.* **72**, 2721 (1994).
  - <sup>8</sup> S. Pekker and G. Oszlányi, *Synth. Metals* **103**, 2411 (1999).
  - <sup>9</sup> G.M. Bendele, P.W. Stephens, K. Prassides, K. Vavakis, K. Kordatos, and K. Tanigaki, *Phys. Rev. Lett.*, **80**, 736 (1998).
  - <sup>10</sup> D. Arçon, K. Prassides, S. Margadonna, A.-L. Maniero, L. C. Brunel, and K. Tanigaki, *Phys. Rev. B* **60**, 3856 (1999).
  - <sup>11</sup> G. Oszlányi, G. Baumgartner, G. Faigel, and L. Forró, *Phys. Rev. Lett.* **78**, 4438 (1997).
  - <sup>12</sup> A. Rezzouk, F. Rachdi, Y. Errammach, and J.L. Sauvajol, *Physica E*, **15**, 107 (2002).
  - <sup>13</sup> M. Yasukawa and S. Yamanaka, *Chem. Phys. Lett.* **341**, 467 (2001).
  - <sup>14</sup> Y. Maniwa, H. Ikejiri, H. Tou, M. Yasukawa, and S. Yamanaka, *Synth. Metals* **121**, 1105 (2001).
  - <sup>15</sup> M. Tomaselli, B. H. Meier, M. Riccò, T. Shiroka, and A. Sartori, *Phys. Rev. B* **63**, 113405 (2001).
  - <sup>16</sup> L. Cristofolini, M. Riccò, and R. De Renzi, *Phys. Rev. B* **59**, 8343 (1999).
  - <sup>17</sup> M. Tomaselli, B. H. Meier, M. Riccò, T. Shiroka, and A. Sartori, *J. Chem. Phys.* **115**, 472 (2001).
  - <sup>18</sup> S. Margadonna, D. Pontiroli, M. Belli, T. Shiroka, M. Riccò, and M. Brunelli, *J. Am. Chem. Soc.* **126**, 15032 (2004).
  - <sup>19</sup> H.M. Guerrero, R.L. Cappelletti, D.A. Neumann, and T. Yildirim, *Chem. Phys. Lett.* **297**, 265 (1998).
  - <sup>20</sup> A. Huq, P.W. Stephens, G.M. Bendele, and R.M. Ibberson, *Chem. Phys. Lett.* **347**, 13 (2001).
  - <sup>21</sup> K.-F. Thier, M. Mehring, and F. Rachdi, *Phys. Rev. B* **55**, 124 (1997).
  - <sup>22</sup> R. Tycko, G. Dabbagh, R.M. Fleming, R.C. Haddon, A.V. Makhija, and S.M. Zahurak, *Phys. Rev. Lett.* **67**, 1886 (1991).
  - <sup>23</sup> N. Sato, H. Tou, Y. Maniwa, K. Kikuchi, S. Suzuki, Y. Achiba, M. Kosaka, and K. Tanigaki, *Phys. Rev. B* **58**, 12433 (1998).
  - <sup>24</sup> C.H. Pennington and V.A. Stenger, *Rev. Mod. Phys.*, **68**, 855 (1996).
  - <sup>25</sup> M. Riccò, T. Shiroka, O. Ligabue, M. Belli, D. Pontiroli, G. Ruani, D. Palles and S. Margadonna, in *Proceedings of the International Symposium on Fullerenes, Nanotubes and Carbon Nanoclusters*, edited by P. V. Kamat, D. M. Guldi, F. D'Souza, (Electrochem. Soc., New York, USA) **615**, 463 (2003).
  - <sup>26</sup> H. Kuzmany, R. Pfeiffer, M. Hulman, and C. Kramberger, *Phil. Trans. A: Math. Phys. Eng. Sci.*, **362**, 2375 (2004).
  - <sup>27</sup> H. Kuzmany, B. Burger, and J. Kürti, in *Optical and Electronic Properties of Fullerenes and Fullerene-Based Materials*, edited by J. Shinar, Z.V. Vardeny, Z.H. Kafafi, (Marcel Dekker, New York, 1999).
  - <sup>28</sup> G.B. Adams and J.B. Page, *Phys. Stat. Solid* **226**, 95 (2001).
  - <sup>29</sup> T. Wågberg and B. Sundqvist, *Phys. Rev. B* **65**, 155421 (2002).
  - <sup>30</sup> B. Friedl, C. Thomsen, H.U. Habermeier, and M. Cardona, *Solid State Commun.* **81**, 989 (1992).
  - <sup>31</sup> T. Wågberg, P. Stenmark, and B. Sundqvist, *J. Phys. Chem. Solids* **65**, 317 (2004).
  - <sup>32</sup> J.S. Duclos, R.C. Haddon, S. Glarum, A.F. Heberd, and K.B. Lyons, *Science* **254**, 1625 (1991).
  - <sup>33</sup> M. Kosaka, K. Tanigaki, K. Prassides, S. Margadonna, A. Lappas, C.M. Brown, and A.N. Fitch, *Phys. Rev. B* **59**, R6628 (1999).
  - <sup>34</sup> W. Andreoni, P. Giannozzi, J.F. Armbruster, M. Knupfer, and J. Fink, *Europhys. Lett.* **34**, 699 (1996).
  - <sup>35</sup> M. Riccò, M. Belli, D. Pontiroli, T. Shiroka, G. Ruani, D. Arçon, and S. Margadonna, manuscript in preparation.